JMEPEG (2011) 20:394–398
DOI: 10.1007/s11665-010-9694-1

1059-9495/$19.00

Inhibition of Aluminum Alloy Corrosion in 0.5 M Nitric Acid Solution by 4-4-Dimethyloxazolidine-2-thione

Ahmed Y. Musa, Abu Bakar Mohamad, Abdul Amir H. Kadhum, and Yousef Bashir A. Tabal

(Submitted April 9, 2010; in revised form May 25, 2010)

The corrosion inhibition of Al-Alloy (Al2024) in 0.5 M nitric acid solution at 30 °C was achieved using 4-4-dimethyloxazolidine-2-thione (DMT) as a corrosion inhibitor. The electrochemical performance of the DMT was studied by electrochemical impedance spectroscopy (EIS), potentiodynamic polarization measurements, and scanning electron microscopic study (SEM). The results indicated that DMT acts as an inhibitor for Al2024 in 0.5 M nitric acid. Polarization curves indicated that DMT was a mixed-type inhibitor. Inhibition efficiencies were observed to be increased with an increase in DMT concentration and attains approximately to 93.4% at 2 mM of DMT in 0.5 M nitric acid. The adsorption of DMT model on Al2024 surface obeyed in accordance with Langmuir adsorption isotherm model. The value of the free energy of adsorption ΔG_{ads} indicated that the adsorption of DMT molecule was a spontaneous process and was typical of physical and chemical adsorption.

Keywords aluminum, corrosion testing, surface engineering

1. Introduction

Aluminum is an important subject of research because it is the most abundant metal and the third most abundant element in the earth's crust and easy to handle. Aluminum is an important material for use in many applications, such as for automobiles, aviation, household appliances, containers, and electronic devices due to its low price, high electrical capacity, high energy density and corrosion resistance. The corrosion resistance of aluminum arises from its ability to form a natural oxide film on its surface in a wide variety of media (Ref 1). Nitric acid solution, however, readily attacks aluminum, and in order to reduce the corrosion to safe level, inhibitors are added. Most of the well-known inhibitors investigated for corrosion of steel and aluminum in acidic medium are heterocyclic compounds, mainly containing oxygen, nitrogen, phosphorous, and sulfur atoms and long carbon chain length as well as multiple bonds or aromatic ring in their molecular structure (Ref 1-4). 4-4-Dimethyloxazolidine-2-thione (DMT) has been reported by authors as a corrosion inhibitor for mild steel in 2.5 M H_2SO_4 solution (Ref 5). The aim of this study was to investigate the corrosion inhibition of aluminum alloy in 0.5 M nitric acid solution by DMT at 30 °C using electrochemical impedance spectroscopy (EIS), potentiodynamic polarization measurements, and scanning electron microscopy (SEM).

Ahmed Y. Musa, Abu Bakar Mohamad, Abdul Amir H. Kadhum, and **Yousef Bashir A. Tabal**, Department of Chemical and Process Engineering, Universiti Kebangsaan Malaysia, 43600 Bangi, Selangor, Malaysia. Contact e-mail: ahmed.musa@ymail.com.

2. Experimental Work

The aluminum alloy (Al2024) with elemental composition shown in Table 1 was used as working electrode in this study. The electrode was first mechanically abraded using SiC papers from No. 400, 800, and 1500 until the surfaces appear free from scratches and other apparent defects, then washed with running tap water followed with deionized water, dried with clean tissue, degreased with absolute ethanol, and finally dried at room temperature before immersion in 0.5 M nitric acid (Ref 6). 4-4-Dimethyloxazolidine-2-thione was used as a corrosion inhibitor for this test. The structural formula for DMT was shown in Fig. 1.

Measurements were carried out in aerated, non-stirred 0.5 M nitric acid solution at 30 °C. Electrochemical experiments were carried out in a glass cell with a capacity of 175 mL. The cell was water jacketed with a graphite electrode of approximately 5 mm diameter used as a counter electrode and a saturated electrode as a reference electrode (SCE). The latter was connected through a Luggin's capillary to the cell. The working electrode was in the form of cylindrical shape with an exposure surface of 4.52 cm^2 and was embedded in a Teflon rod and immersed in a test solution until steady state open-circuit potential (OCP) was noted. All the test solutions were prepared from analytical-grade chemical reagents in distilled water. Electrochemical measurements were performed using Gamry Instrument Potentiostat/Galvanostat/ZRA, Gamry applications that include OCP, potentiodynamic scan, and EIS are comprised in DC105 and EIS300 software. The potentiodynamic current-potential curves were recorded by changing the electrode potential automatically from −200 to 200 mV versus OCP with scan rate of 1 mV s^{-1}. The impedance measurements were performed at corrosion potential over a frequency range of 10 kHz to 0.1 Hz, with a signal amplitude perturbation of 10 mV. All impedance data were fitted to appropriate equivalent circuits (EC) using Gamry Echem Analyst software. Experiments for

Table 1 Composition of the aluminum alloy (Al2024)

Element	Content, wt.%
Cu	3.8
Cr	0.1
Fe	0.5
Mg	1.2
Mn	0.3
Si	0.5
Ti	0.15
Zn	0.25
Al	Remainder

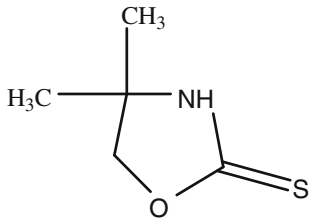

Fig. 1 The molecular structure of DMT

electrochemical measurements were started about 120 min after the working electrode was immersed in solution to allow a stabilization of the steady state potential.

3. Results and Discussion

3.1 Electrochemical Impedance Spectroscopy (EIS) Measurements

Nyquist plots for Al2024 in 0.5 M nitric acid in the absence and presence of various concentrations of the DMT were shown in Fig. 2. A considerable increase in the total impedance can be observed clearly in the recorded Nyquist plots with the increase of inhibitor concentration. It's clearly that Nyquist plots were characterized by a large depressed semicircular capacitive loop at high frequency which is then followed by small inductive loops at low frequencies. The obtained semicircles either in absence or in presence of inhibitor were depressed. Deviations of this kind are referred to frequency dispersion, have been attributed to inhomogeneties of solid surfaces of the Al surface (Ref 7). The high frequency capacitive loop could be assigned to the relaxation process in the aluminum oxide film presents on the aluminum surface and its dielectric properties. While the presence of the inductive loop suggests that the passivated surface was re-dissolved at low frequencies (Ref 8). The appearance of the inductive loop for all inhibited systems indicates that the studied inhibitors do not affect the anodic process. The equivalent circuit model employed for this system is shown in Fig. 3. This consists of constant phase element (CPE) in parallel to the parallel resistors of charge transfer (R_{ct}) and layer resistor (R_L), and the latter is in series with the inductor (L) due to the inductive loop. Figure 4 represents the fitted experimental data of EIS for nitric acid solution in the

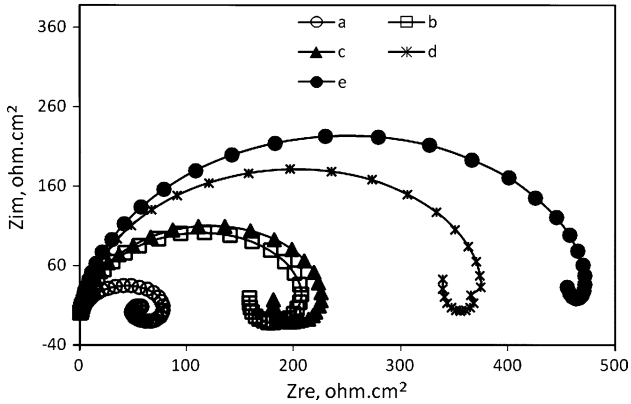

Fig. 2 Nyquist plots for Al2024 in 0.5 M nitric acid solution at 30 °C in the absence (a) and the presence (b) 0.1 mM, (c) 0.5 mM, (d) 1 mM, and (e) 2 mM of DMT

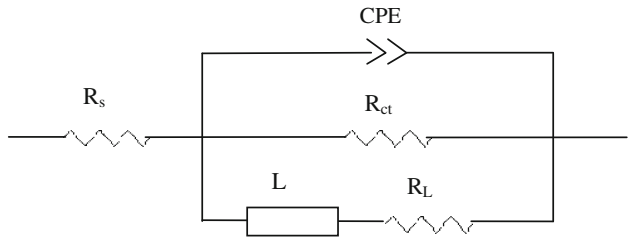

Fig. 3 Equivalent circuit model used to fit the experimental data

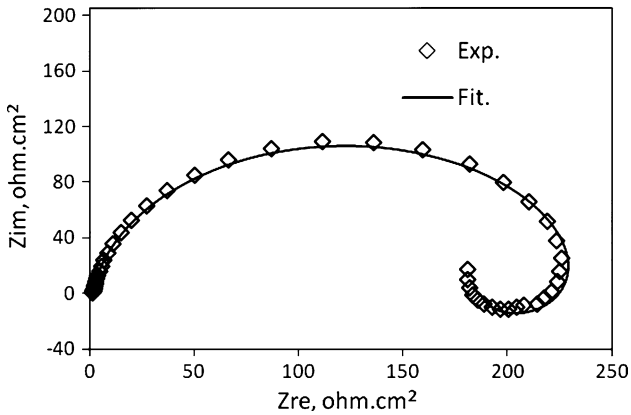

Fig. 4 EIS-fitted data for Al2024 in 0.5 M nitric acid solution with 0.5 mM of DMT using the equivalent circuit model in Fig. 3

presence of inhibitor using the equivalent circuit in Fig. 3. CPE is defined in impedance representation as (Ref 2):

$$Z(\omega) = Z_0 \cdot (j\omega)^{-n} \quad \text{(Eq 1)}$$

where Z_0 is the CPE constant, ω is the angular frequency (in rad/s), $j^2 = -1$ is the imaginary number, and n is the CPE exponent.

The fitted values were depicted in Table 2. As seen from Table 2, the R_{ct} values increased with the DMT concentration, which can be attributed to the formation of a protective over layer at the Al surface, which becomes a barrier for the

mass and the charge transfers. The inhibition efficiency IE% was calculated by charge transfer resistance (R_{ct}) as follows (Ref 2):

$$IE\% = \frac{R_{ct} - R_{ct}^0}{R_{ct}} \times 100 \quad \text{(Eq 2)}$$

where R_{ct} and R_{ct}^0 are the charge transfer resistances with and without DMT, respectively.

It was found that the inhibition efficiency increases with increasing of concentration inhibitor. The Bode plots as presented in Fig. 5 were plotted using the same experimental data in the Nyquist format. It shows a new phase angle shift at higher frequency range with inhibitor concentration of 0.1 mM. This new phase shift means that the addition of DMT changed the electrode interfacial structure, and resulted in an extra time constant and the creation of the film forming on electrode surface (Ref 9).

Table 2 Fitted impedance parameters of Al2024 in 0.5 M HNO_3 in the absence and the presence of different concentrations of DMT at 30 °C

Inhibitor concentration, mM	R_{ct}, ohm cm^2	C_{dl}, µF cm^{-2}	IE%
Blank	80.49	12.95	…
0.1	223.2	30.53	63.93
0.5	243.9	42.17	66.99
1.0	405.5	43.93	80.15
2.0	692.6	55.43	88.37

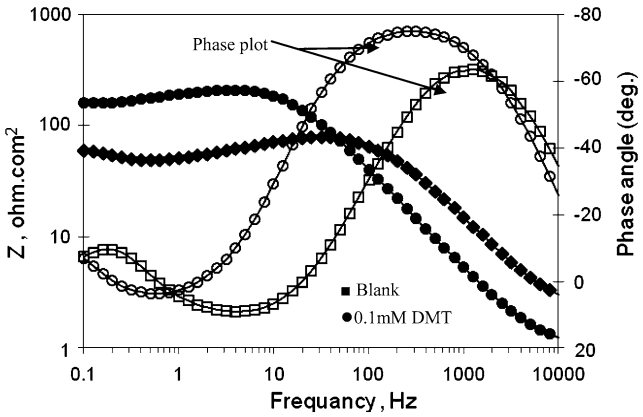

Fig. 5 Bode plots for Al2024 in 0.5 M nitric acid solution with and without DMT

3.2 Polarization Measurements

Potentiodynamic polarization scan was carried out at 30 °C in 0.5 M nitric acid with different concentrations of DMT. Polarization curves in the absence and in the presence of different concentrations of inhibitor were shown in Fig. 6. In general, the presence of increasing amount of the DMT leads to a dramatical decrease in the cathodic current density associated with limited increase in the anodic current density. However, the inhibited system was shifted toward cathodic potentials, emphasizing that the DMT acts as a cathodic inhibitor. This result is in good agreement with that obtained from impedance measurements. The numerical values of anodic (β_a) and cathodic (β_c) Tafel constants, corrosion current densities (i_{corr}), and corrosion potential (E_{corr}) are listed in Table 3. These values were calculated from the Tafel fit routine provided by Gamry Echem. Analyst software; this routine uses a non-linear chi-squared minimization to fit the data to the Stern-Geary equation. The surface coverage (θ) was calculated using the following formulas (Ref 2):

$$\theta = \frac{i_{corr(uninh)} - i_{corr(inh)}}{i_{corr(uninh)}} \quad \text{(Eq 3)}$$

where $i_{corr(uninh)}$ and $i_{corr(inh)}$ are the corrosion current densities in the absence and the presence of DMT, respectively.

In order to confirm the impedance results, the inhibition efficiency (IE%) of DMT was calculated as follows (Ref 2):

$$IE\% = \theta \times 100 \quad \text{(Eq 4)}$$

It was observed from Table 3 that i_{corr} decreased with increasing DMT concentration while the inhibition efficiencies

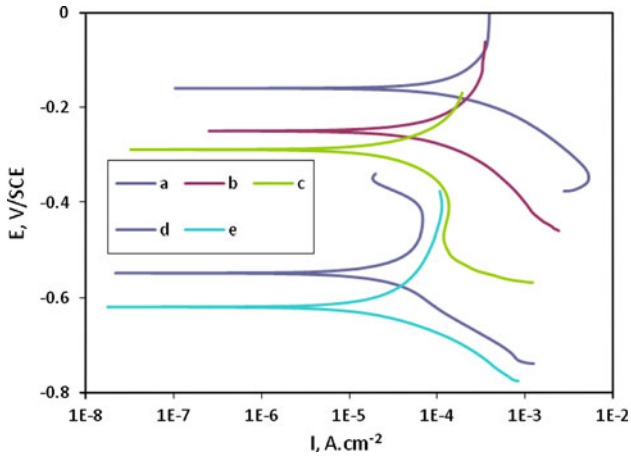

Fig. 6 Potentiodynamic polarization curves for Al2024 in 0.5 M nitric acid solution at 30 °C in absence (a) and presence (b) 0.1 mM, (c) 0.5 mM, (d) 1 mM, and (e) 2 mM of DMT

Table 3 Polarization parameters of Al2024 in 0.5 M HNO_3 in absence and presence of different concentration of DMT at 30 °C

Inhibitor concentration, mM	β_a, V dec^{-1}	β_c, V dec^{-1}	i_{corr}, µA cm^{-2}	E_{corr}, mV vs. SCE	θ	IE%
Blank	0.269	0.103	248	−159	…	…
0.1	0.127	0.101	82.7	−250	0.666	66.6
0.5	0.116	0.930	28.9	−288	0.883	88.3
1.0	0.112	0.898	27.0	−548	0.891	89.1
2.0	0.109	0.639	16.4	−620	0.934	93.4

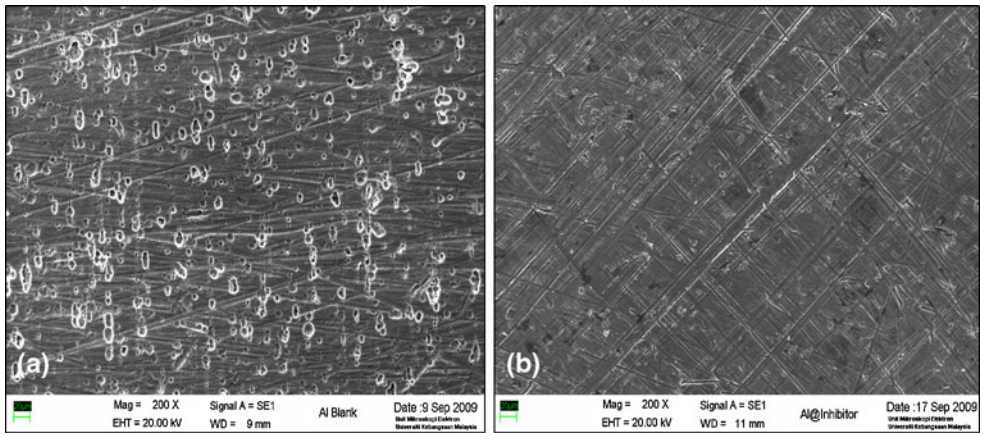

Fig. 7 SEM images of the Al2024 surface after immersion in 0.5 M nitric acid solution for 6 h in the absence (a) and presence (b) of DMT

increased with the concentration of DMT. The addition of DMT shifted E_{corr} values toward more negative values, indicating the inhibiting effect of DMT on Al2024 and indicating a cathodic control mechanism. The calculated values of inhibition efficiencies of DMT obtained by potentiodynamic polarization are in good agreement with those obtained by EIS measurements.

3.3 Scanning Electron Microscopy (SEM)

In order to establish the formation of protective layer on the Al surface, scanning electron microscopic images were taken. The Al2024 surface images after immersion in 0.5 M nitric acid solution in the absence and the presence of DMT for 6 h are shown in Fig. 7. The photomicrograph of the Al2024 without inhibitor showed some cracks and pits due to the attack of corrosive solution while in the presence of 2 mM DMT; there are no cracks and pits observed in the micrograph except polishing lines; also, a uniform modification of the Al2024 surface is observed, which is due to the protective film formed by DMT on the Al2024 surface.

3.4 Adsorption Isotherms

The adsorption isotherm can provide basic information for the nature of processes between inhibitor and metal surface (Ref 10). The degrees of surface coverage (θ) of different concentrations of DMT in 0.5 M nitric acid were calculated from polarization measurements. Assumed that the system follows Langmuir adsorption isotherm, which is given by Eq 5 (Ref 2).

$$\frac{C_{inh}}{\theta} = \frac{1}{K_{ads}} + C_{inh} \quad \text{(Eq 5)}$$

where C_{inh} is the inhibitor concentration, and K_{ads} the equilibrium constant of the adsorption/desorption process. The plot of C_{inh}/θ versus C_{inh}, yielded a straight line, Fig. 8, with correlation coefficient of (0.999) which close to unity with slope of 1.050, provided that the adsorption of DMT from 0.5 M nitric acid solution on the Al surface obeys Langmuir adsorption isotherm. The value of equilibrium constant (K_{ads}) is calculated from the reciprocal of the intercept of isotherm line as 9522.9 M^{-1}. The high value of adsorption equilibrium constant shows that DMT is strongly adsorbed on the Al2024

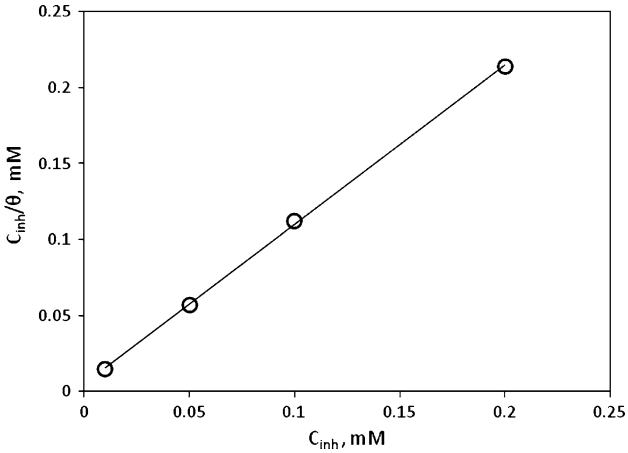

Fig. 8 Adsorption isotherm for DMT molecules on Al2024 surface in 0.5 M nitric acid solution at 30 °C

Table 4 Adsorption parameter of inhibitor for Al2024 in 0.5 M HNO_3 at 30 °C

Slope	R^2	K_{ads}, M^{-1}	ΔG_{ads}, kJ mol^{-1}
1.050	0.999	9522.9	−33.197

surface (Ref 11). The adsorption free energy (ΔG_{ads}) of inhibitor on Al2024 surface can be evaluated using the following Eq 5 (Ref 12):

$$\Delta G_{ads} = -RT \ln(55.5 K_{ads}) \quad \text{(Eq 6)}$$

where R is the gas constant (8.314 J K^{-1} mol^{-1}), T is the absolute temperature (K), and the value, 55.5, in the above equation is the concentration of water in solution in M (Ref 13). The value of ΔG_{ads} is calculated and presented in Table 4.

The negative value of ΔG_{ads} ensured that the spontaneity of the adsorption process, stability of the adsorbed layer on the Al2024 surface, and also a strong interaction between inhibitor molecules and Al2024 surface (Ref 12). In general, values of ΔG_{ads} up to −20 kJ mol^{-1} are consistent with electrostatic interaction between charged molecules and a charged metal

(which indicates physical adsorption) while, the value of ΔG_{ads} for chemisorption is close to or more negative than -40 kJ mol^{-1}. Such a value implies either transfer of electrons or sharing with inhibitor molecules on the metal surface (Ref 2). The calculated ΔG_{ads} value indicating that the adsorption mechanism of DMT on Al2024 in studied acid media at 30 °C was in both physical and chemical adsorption (Ref 14).

4. Conclusion

4-4-Dimethyloxazolidine-2-thione (DMT) has been proved to be efficient as corrosion inhibitor for aluminum alloy (Al2024) in 0.5 M nitric acid solution. The inhibition efficiency was observed to be increased with DMT concentration. The polarization curves indicated that DMT was a cathodic inhibitor. Scanning electron microscopy (SEM) revealed the formation of a smooth, dense protective layer on Al surface in the presence of DMT. The adsorption of DMT on the Al2024 surface was spontaneous and was best described by Langmuir adsorption isotherm. Based on the value of the free energy ΔG_{ads} obtained, the mechanism of adsorption of DMT was physical and chemical adsorption.

Acknowledgment

The authors gratefully acknowledge the Universiti Kebangsaan Malaysia for the support of this project under Grant No. UKM-GUP-BTT-07-25-170.

References

1. E.M. Sherif and S.-M. Park, Effects of 1,4-Naphthoquinone on Aluminium Corrosion in 0.50 M Sodium Chloride Solutions, *Electrochim. Acta*, 2006, **51**, p 1313–1321
2. A.Y. Musa, A.A.H. Khadum, A.B. Mohamad, M.S. Takriff, A.R. Daud, and S.K. Kamarudin, On the Inhibition of Mild Steel Corrosion by 4-Amino-5-phenyl-4H-1,2,4-trizole-3-thiol, *Corros. Sci.*, 2010, **52**, p 526–533
3. A.Y. Musa, A.A. Khadom, A.A.H. Khadum, A.B. Mohamad, and M.S. Takriff, Kinetic Behavior of Mild Steel Corrosion Inhibition by 4-Amino-5-phenyl-4H-1,2,4-trizole-3-thiol, *J. Taiwan Inst. Chem. Eng.*, 2010, **41**, p 126–128
4. A.Y. Musa, A.A.H. Kadhum, M.S. Takriff, A.R. Daud, and S.K. Kamarudin, Evaluation of Ethylenediaminetetra-Acetic Acid Di-Sodium Salt as Corrosion Inhibitor for Mild Steel in 1 M Hydrochloric Acid, *Aust. J. Basic Appl. Sci.*, 2008, **2**, p 956–960
5. A.Y. Musa, A.A.H. Kadhum, A.B. Mohamad, A.R. Daud, M.S. Takriff, and S.K. Kamarudin, A Comparative Study of the Corrosion Inhibition of Mild Steel in Sulphuric Acid by 4,4-Dimethyloxazolidine-2-thione, *Corros. Sci.*, 2009, **51**, p 2393–2399
6. ASTM Standard G1-3, *Standard Practice for Preparing, Cleaning, and Evaluating Corrosion Test Specimens*, ASTM International, West Conshohocken, PA, 2003. doi:10.1520/G0001-03
7. A. Despic and V.P. Parkhutik, *Modern Aspects of Electrochemistry*, Vol 20, Plenum Press, New York, 1989, p 401
8. E.A. Noor, Evaluation of Inhibitive Action of Some Quaternary N-heterocyclic Compounds on the Corrosion of Al-Cu Alloy in Hydrochloric Acid, *J. Mater. Chem. Phys.*, 2009, **114**, p 533–541
9. A.Y. Musa, A.A.H. Kadhum, M.S. Takriff, A.R. Daud, S.K. Kamarudin, and N. Muhamad, Corrosion Inhibitive Property of 4-Amino-5-phenyl-4H-1,2,4-triazole-3-thiol for Mild Steel Corrosion in 1.0 M Hydrochloric Acid, *Corros. Eng. Sci. Technol.*, 2010, **45**, p 163–168
10. R. Solmaz, M.E. Mert, G. Kardaş, B. Yazici, and M. Erbıl, Adsorption and Corrosion Inhibition Effect of 1,1′-Thiocarbonyldiimidazole on Mild Steel in H_2SO_4 Solution and Synergistic Effect of Iodide Ion, *Acta Phys. Chim. Sin.*, 2008, **24**, p 1185–1191
11. G. Avci, Corrosion Inhibition of Indole-3-acetic Acid on Mild Steel in 0.5 M HCl, *Colloids Surf. A: Physicochem. Eng. Asp.*, 2008, **317**, p 730–736
12. M. Abdallah, Rhodanine Azosulpha Drugs as Corrosion Inhibitors for Corrosion of 304 Stainless Steel in Hydrochloric Acid Solution, *Corros. Sci.*, 2002, **44**, p 717–728
13. M.A. Amin, S.S. Abd EI-Rehim, E.E.F. El-Sherbini, O.A. Hazzazi, and M.N. Abbas, Polyacrylic Acid as a Corrosion Inhibitor for Aluminium in Weakly Alkaline Solutions. Part I. Weight Loss, Polarization, Impedance EFM and EDX Studies, *Corros. Sci.*, 2009, **51**, p 658–667
14. X.Y. He, H.Y. Deng, R. Li, X.D. Fei, H.Y. Wang, and Z.Y. Deng, Corrosion Inhibition of X70 Steel in Saline Solution Saturated with CO_2 by Thiourea, *Acta Metall. Sin. (Engl. Lett.)*, 2008, **21**, p 65–71